Profiling of Chemonaive Osteosarcoma and Paired-Normal Cells Identifies EBF2 as a Mediator of Osteoprotegerin Inhibition to Tumor Necrosis Factor–Related Apoptosis-Inducing Ligand–Induced Apoptosis

Ana Patiño-García,[1] Marta Zalacain,[1] Cecilia Folio,[1,5] Carolina Zandueta,[5] Luis Sierrasesúmaga,[1,2] Mikel San Julián,[3] Gemma Toledo,[4] Javier De Las Rivas,[6] and Fernando Lecanda[5]

Laboratories of [1]Pediatrics and [2]Pediatric Oncology and Departments of [3]Orthopedics and [4]Pathology, University Hospital; [5]Division of Oncology, Adhesion and Metastasis Laboratory, Center for Applied Biomedical Research, University of Navarra, Pamplona, Spain and [6]Bioinformatics and Functional Genomics Research Group, Cancer Research Centre and University of Salamanca, Salamanca

ABSTRACT

Purpose: Osteosarcoma is the most prevalent bone tumor in children and adolescents. At present, the mechanisms of initiation, maintenance, and metastasis are poorly understood. The purpose of this study was to identify relevant molecular targets in the pathogenesis of osteosarcoma.

Experimental Design: Tumor chemonaive osteoblastic populations and paired control normal osteoblasts were isolated and characterized phenotypically from seven osteosarcoma patients. Global transcriptomic profiling was analyzed by robust microarray analysis. Candidate genes were confirmed by real-time PCR and organized in molecular pathways. EBF2 and osteoprotegerin (OPG) levels were determined by real-time PCR and OPG protein levels were assessed by ELISA. Immunohistochemical analysis was done in a panel of 46 osteosarcoma samples. Silencing of EBF2 was achieved by lentiviral transduction of short hairpin RNA. Apoptosis was determined by caspase-3/7 activity.

Results: A robust clustered transcriptomic signature was obtained in osteosarcoma. Transcription factor EBF2, a known functional bone regulator, was among the most significantly overexpressed genes. Immunohistochemical analysis showed that osteosarcoma is expressed in □70% of tumors analyzed. Because EBF2 was shown previously to act as a transcriptional activator of OPG, elevated levels of EBF2 were associated with high OPG protein levels in osteosarcoma samples compared with normal osteoblastic cells. Knockdown of EBF2 led to stunted abrogation of OPG levels and increased sensitivity to tumor necrosis factor-related apoptosis-inducing ligand (TRAIL)–induced apoptosis.

Conclusions: These findings suggest that EBF2 represents a novel marker of osteosarcoma. EBF2 up-regulation may be one of the mechanisms involved in the high levels of OPG in osteosarcoma, contributing to decrease TRAIL-induced apoptosis and leading to TRAIL resistance.

INTRODUCTION

Osteosarcoma is the most common primary malignant tumor of bone characterized by production of osteoid and a high propensity to metastasize (1). It most frequently occurs in the second decade of life with □60% of patients ages <25 years, whereas 30% of osteosarcoma occurs in patients ages >40 years.

At present, the standard treatment for high-grade osteosarcoma includes neoadjuvant chemotherapy followed by surgical resection and postoperative chemotherapy. Several clinical factors have been related to survival, including the presence of metastatic disease and the histologic response to preoperative chemotherapy. Despite the efforts in new therapeutic modalities, survival remains □65% to 70% in patients with nonmetastatic disease (2, 3).

Osteogenic sarcoma affecting children and adolescents mostly includes sporadic cases of unknown etiology, with a peak of incidence during the pubertal growth spurt. In this group of classic, high-grade osteosarcoma, few, if any, genetic alterations are present in a substantial subset of these tumors and the frequency of the alterations usually varies between studies depending on the design and the specimens included (4). About 70% of osteosarcomas have altered karyotypes, being the gain of chromosome 1, loss of 9, 13 (RB1 gene), and 17 (TP53), and structural aberrations affecting chromosomes 11, 19, and 20 the most frequently encountered chromosomal aberrations (5–7).

Histologically, the predominant cell type displays typical osteoid secretion, with different degrees of fibroblastic and osteochondroblastic components. This cellular heterogeneity arises from the high plasticity of the mesenchymal cell lineage from which mature osteoblasts derive through a tightly regulated process (8) driven by several factors, which induce the expression of bone markers including osteocalcin, and several bone matrix proteins including collagen type I, osteopontin, and bone sialoprotein (9).

At present, global transcriptomic profiling of human osteosarcoma remains highly divergent among studies (10–13). Several major explanations could account for these conflicting findings. First, most of the studies rely on surgical specimens, or paraffin-embedded material, where the tumor remains surrounded by nontumoral cells, including inflammatory components, which highly influence transcriptomic profiling. Second, surgical specimens most frequently represent advanced lesions in which chromosomal instability leads to a heterogeneous constellation of cytogenetic alterations within the same tumor. Third, some of the studies have been done using commercial cell lines, which do not totally recapitulate all features of the original tumor from which they were derived. Fourth, several of the studies include specimens belonging to different etiopathologic subgroups.

To overcome these limitations, we have focused on the classic high-grade, sporadic osteosarcoma cases and we have undertaken a different approach by isolating and characterizing several human chemonaive cell populations derived from primary osteosarcomas and their paired-normal primary osteoblastic counterparts. With the long-term goal of understanding the molecular mechanisms and to unveil commonly altered molecular pathways, we have used this set of samples to perform global transcriptomic profiling. Using this approach, we found a robust clustering that revealed a novel gene subset that was further validated by quantitative real-time PCR (RT-PCR). A frequent alteration in the mechanisms of apoptosis was observed in tumor cells. We identified

and functionally validated EBF2 as a pathway altered in osteosarcoma. Functional assays showed a common resistance to tumor necrosis factor (TNF)–related apoptosis-inducing ligand (TRAIL)–mediated apoptosis. Elevated levels of the transcription factor EBF2 in tumor cells were correlated with high levels of osteoprotegerin (OPG) presumably by direct binding to its promoter (14). In turn, increased levels of this decoy receptor accounted for the resistance to TRAIL-mediated apoptosis. These findings identified EBF2 as a novel marker of osteosarcoma and revealed a novel mechanistic insight into the resistance to apoptosis, which could have clinical implications.

TRANSLATIONAL RELEVANCE

The mechanisms of osteosarcoma pathogenesis are largely unknown. Here we identified EBF2, a known transcription factor of osteoprotegerin (OPG), as a relevant marker up-regulated in osteosarcoma. Silencing of EBF2 led to a concomitant decrease in OPG levels in osteosarcoma cells and a decreased resistance to apoptosis induced by tumor necrosis factor–related apoptosis–inducing ligand. These findings involve EBF2 up-regulation as one of the mechanisms contributing to high OPG levels in osteosarcoma. It might be possible to use EBF2 as a novel target in combination with anti–tumor necrosis factor–related apoptosis-inducing ligand therapy to increase the clinical benefit in osteosarcoma patients.

MATERIALS AND METHODS

Patients and clinical samples

Primary tumor samples were obtained by needle biopsy from seven high-grade osteosarcomas before induction chemotherapy, and paired-normal osteoblasts were isolated when patients underwent surgery. Small (1 X 1 X 0.5 cm) biopsies of normal trabecular bone were obtained beyond the marginal resection border (Table 1). All patients were treated at the Pediatric Oncology Unit of the University Hospital of Navarra. All the samples were obtained with written informed consent from patients and/or their parents and the protocol was approved by the local ethics committee.

Human osteoblasts were isolated according to procedures we have published previously (9). Briefly, needle biopsy specimens were cleaned of soft tissue under a dissecting microscope. The remaining bone chips were washed with PBS and treated with 250 units/mL collagenase and DNase in α-MEM for 2 h. Following digestion, bone debris were separated by using a 70 μm nylon mesh. Cells were precipitated by centrifugation, washed several times to remove excess collagenase and DNase, and placed in α -MEM containing 10% heat-inactivated fetal bovine serum, 100 units/mL penicillin, and 100 μg/mL streptomycin. The remaining bone chips were also cultured in the same medium. After 4 weeks, outgrowing osteoblasts were subcultured and characterized. All experiments were done with 1 to 5 passages normal osteoblastic cells, whereas tumoral cells were passed between 20 and 40 times; in all cases, cells were 90% confluent and in logarithmic growth phase. Small fractions of cells were routinely seeded and histochemical determination of alkaline phosphatase activity was done. The cell lines derived from the tumors were designed as the number of the patient followed by B (biopsy) and the paired-normal cell lines by N (normal).

Characterization of the osteoblastic phenotype

All normal and tumor-derived cell lines were tested for the expression of alkaline phosphatase (Sigma-Aldrich). Additional markers of the osteoblastic lineage, collagen α1 type I, osteopontin, bone sialoprotein, and osteocalcin, were tested by semiquantitative RT-PCR using previously described primers and conditions (15).

Tumorgenotypic characterization

Tumor-derived and normal bone cell lines were checked for mutations in genes that are frequently mutated in osteosarcoma. Exons 5 to 9 of TP53 were analyzed by direct sequencing of the PCR products and loss of heterozygosity was determined by the analysis of a VNTR marker located in intron 1 of the gene. Loss of heterozygosity at the RB1 gene was determined by the use of repeat polymorphisms located in introns 2 (D13S153) and 20 (Rb1.20) of the gene and comparison of the allele patterns in normal and tumor samples.

Proliferation and apoptosis assay

Cell proliferation was assessed by MTT assay according to the manufacturer's recommendations (Roche Applied Science). Cells were seeded in 96-well plates at a cell density of 10^3 per well and then cultured for 2, 4, and 6 days. Apoptosis was analyzed in triplicate assays with the Caspase-Glo-3/7 Assay (Promega Biotech Ibérica). Briefly, 1,000 cells per well were seeded in 96-well plates, and after incubation with α-MEM supplemented with 0.4% fetal bovine serum for 24 h, the assay was initiated. Cells were incubated for 24 h with TNF-α (25 ng/mL), TRAIL (50 ng/mL), and OPG (1 μg/mL) or their combination. After incubation, luminescence of each sample was measured in a plate-reading luminometer (Sunrise Remote) at 485/527 nm. Results were plotted as the mean signal-to-noise ratios of the triplicate assays. Experiments were repeated three times.

RNA extraction for microarray analysis

RNA was isolated from 1 X 10^6 cells in logarithmic growth phase using the Qiagen RNeasy Mini Kit. Quality of the RNA was determined with a bioanalyzer (2100; Agilent Technologies) and the amount of RNA was established using a spectrophotometer (NanoDrop). Samples were stored at -80°C until RNA hybridization. Labeling and hybridization of the HG-U133A chips were done by Progenika Biopharma. The set corresponds to 14 samples (7 control bones and 7 osteosarcomas) derived from human osteosarcoma populations and their paired osteoblast control cells were obtained from the same patients.

Microarray data analysis: normalization, signal calculation, significant differential expression, and sample/gene profiles clustering

Microarray data analysis was done using the following strategy and methods: RMA algorithm was used for background correction, intra- and intermicroarray normalization, and expression-signal calculation (16–18). Once calculated, the absolute expression

signal for each gene (the signal value for each probe-set) in each microarray, significance analysis of microarrays method (19), was applied to calculate significant differential expression and find the gene probe-sets that characterized the osteosarcoma samples. The method uses permutations to achieve robust statistical inference of the most significant genes and provides P values adjusted to multiple testing using false discovery rate (19). A cutoff of false discovery rate < 0.05 was used for all the differential expression calculations (20).

Following selection of the differentially expressed gene probe-sets, the corresponding matrix of expression values from all microarray hybridization samples (14 in total) was analyzed using the HCLUST clustering algorithm (21). This algorithm performs hierarchical cluster analysis with complete linkage to find similar expression profiles between gene probe-sets based on their correlation values along all the sample microarrays analyzed (calculated using the Pearson correlation coefficient). This is a semisupervised classification because only the genes with significant differential expression are included in HCLUST algorithm. We applied all these methods using R[7] and Bioconductor as main computational and bioinformatic tools.[8]

Gene expression validation by Micro Fluidic Cards

To validate the results obtained, we performed TaqMan verification for expression of 96 selected genes in all 14 cell lines used in the previous experiments and 14 additional samples (5 normal and 9 tumoral) using an Applied Biosystems 7900HT Micro Fluidic Card System (Applied Biosystems). For the design of the test plates, probes were selected as partially overlapping with the Affymetrix probe-sets or at a 100-bp distance avoiding, when possible, intronic sequences. These criteria were fulfilled in 41 of 96 designed probes. For some genes (TLE3, PCBP1, PCBP2, EBF2, PHLDA1, OPG, and ADNP), gene expression was additionally tested by conventional semiquantitative RT-PCR in the same battery of osteosarcoma cell samples. Estimation of mRNA levels was done relative to GAPDH as an internal reference in all cases and the quantity of starting material and the number of PCR cycles were optimized to ensure product yield within the linear range of amplification.

Gene expression validation by quantitative RT-PCR with TaqMan probes

Total RNA was isolated from confluent cultures using Trizol RNA (2 μg), DNase I treated, and reverse transcribed using SuperScript II reverse transcriptase and random primers. For RT-PCR analysis of the gene expression, 1:80 dilution of this reaction was used with SYBR Green I dye chemistry. PCR product was monitored using a Gene Amp 7300 sequence detection system (Applied Biosystems). The mean cycle threshold value (Ct) from triplicate samples was used to calculate gene expression. PCR products were normalized to GAPDH levels (22). Primers for OPG and EBF2 were obtained from Assay-on-Demand (Applied Biosystems).

Lentiviral transduction

Lentiviral vectors containing short hairpin RNA for EBF2 were obtained from shRNA Mission (Sigma). To obtain viral particles, packaging cells were transfected with 8 μg DNA for each construct by calcium phosphate method. Empty vector was used to obtain

mock infective viral particles. Two days after transfection, supernatants were centrifuged for 10 min at 600 × g and filtered through 0.45 μm pore cellulose acetate filter. For transduction infection, 595B cells were seeded at 1 X 10^5 and incubated overnight with viral supernatants in the presence of 4 μg/mL polybrene (Sigma). Forty-eight hours post-infection, cell populations were incubated in medium containing the appropriate antibiotic for 2 additional weeks. Antibiotic-resistant pools were expanded and frozen at each cell passage.

Immunohistochemistry

Osteosarcoma tissue microarray was developed using archival samples of the University Hospital in our institution. The tissue microarray contains 233 tissue spots derived from 46 patients. It includes normal bone (17.2%), osteosarcomas at diagnosis (26.3%), after induction with chemotherapy (11.1%), relapsed tumors (10.1%), and metastasis (35.4%). Formalin-fixed, paraffin-embedded tissue sections were used for the immunohistochemical procedures. Paraffin was removed from the tissues and the sections were hydrated through a graded series of ethanol. Endogenous peroxidase activity was quenched with 3% hydrogen per-oxidase for 10 min. Microwave antigen retrieval was carried out with EDTA (0.5 mmol/L, pH 8) for 2 × 15 min. Nonspecific binding sites were blocked with 5% goat normal serum in TBS-Tween 20 (washing buffer; DAKO) for 30 min. Sections were incubated with anti-EBF2 antibody (Genway) overnight at 4°C. The working dilution was 1:300. After rinsing with TBS, sections were incubated with polyclonal Envision complex (DAKO). The peroxidase activity was shown by 3,3′-diaminobenzidine. Finally, sections were washed in water, lightly counterstained with hematoxylin, dehydrated, and mounted in DPX.

Statistical analysis

Gene expression levels were compared with the Mann-Whitney U test or the Kruskal-Wallis test. The statistical analysis was done with the SPSS software version 15.0 (Statistical Package for the Social Sciences). In all cases, statistical significance was defined as $P < 0.05$.

RESULTS

Isolation and characterization of chemonaive cell populations

Tumor cell populations were obtained from patients diagnosed with high-grade osteosarcoma. Clinical features of the patients are summarized in Table 1. This subset included tumors with different degree of histologic differentiation (Fig. 1A). In all cases, cultures were successfully obtained at diagnosis from a “true-cut” needle biopsy of 0.5 mm. Tumor cells were isolated, amplified, and cultured from 15 to 22 passages, whereas normal osteoblasts were subjected to <5 passages (Fig. 1B).

To characterize the isolated subpopulations, we screened for classic altered genes, TP53 and RB1. In 2 of the 7 tumor samples, we detected alterations in TP53. These alterations included a sample with a hemizygous deletion plus a mutation in exon 8 (C277Y). The other tumor showed a hemizygous deletion plus a mutation in exon 7 (S241Y; Supplementary Fig. S1).

Microscopic examination revealed heterogeneous morphology among different tumor cell lines (Fig. 1B). To test the degree of osteoblastic differentiation, genes of the osteoblastic phenotype were tested by semiquantitative RT-PCR in both normal and tumor-derived cell lines. In all cases, we detected expression of collagen α1 type I, osteopontin, bone sialoprotein, and osteocalcin in all cell lines. However, the expression of osteocalcin was decreased in tumors cells compared with paired-normal osteoblasts (Supplementary Fig. S2). On incubation with 1,25-dihydroxyvitamin D_3, similar levels of osteocalcin were reached compared with normal osteoblasts (data not shown). Similarly, alkaline phosphatase activity was also lower in primary tumor cell lines compared with normal bones (Supplementary Fig. S2). These data suggest that tumor-derived cell lines represent populations of the osteoblastic lineage, which display a perturbed differentiation program.

Proliferation and apoptosis

To explore the mechanisms of growth and resistance, we examined the proliferation and resistance to apoptosis of transformed cells compared with paired-normal osteoblasts. MTT assay revealed that cell kinetics differed among samples. Several samples tumor cell populations showed a lower proliferation than paired-normal osteoblasts (Supplementary Fig. S3). More importantly, apoptosis stimuli, either by incubation in serum-free medium or with VP-16, a DNA damage compound (23), induced cell death in both tumor and normal cell lines. However, tumor-derived cell populations displayed different levels of resistance to apoptosis than paired-normal osteoblasts (data not shown). These findings indicate that transformed cells showed altered mechanisms of cell proliferation and apoptosis.

Global transcriptomic profiling

Stringent bioinformatic processing revealed a robust set of differentially expressed significant genes, including 136 gene probe-sets that corresponded to 122 distinct human genes, which had a fold-change ratio above 2.8 times for the up-regulated and below 2.8 times for the down-regulated. The selected 136 gene probe-sets were used to perform a semisupervised clustering with all the 14 samples that revealed clear profiles with 116 overexpressed and 20 repressed gene probe-sets in the tumor samples. To represent the data in a heat map (Fig. 2), we only included 105 gene probe-sets that corresponded to known annotated human genes. In this clustering, 87 gene probe-sets were over-expressed in the tumor samples and 18 were repressed. A complete list of the identities of these genes can be found in Supplementary Table S1.

To confirm the involvement of the selected genes in osteosarcoma carcinogenesis, we performed TaqMan verification for expression of 96 selected genes in a total of 28 samples: 14 cell lines used in the previous experiments and 14 additional samples (5 normal, 4 primary tumor, and 5 osteosarcoma lung metastases). In the list of genes, 93 were target genes, 4 of which were excluded due to absence of amplification (CPS1,

HNF4A, PDE4C, and NR2E1) and 3 were housekeeping genes used for normalization: GAPDH, RER1, and DNCL2A. The genes that were validated (associated $P < 0.05$) or that showed a tendency to be involved in the model (associated $P = 0.05$-0.09) are included in Table 2.

For some genes (TLE3, PCBP1, PCBP2, TNFRSF6, EBF2, OPG, PHLDA1, and ADNP), gene expression was additionally tested by TaqMan quantitative PCR analysis. In all cases, the result of the validation in the Micro Fluidic Card System was the same when using the gene-by-gene approach. PCBP2, EBF2, and TNFRSF6 genes were overexpressed in osteosarcomas compared with normal samples, whereas PHLDA1 and TLE3 expression were decreased. Expression of PCBP1 and ADNP were unchanged. More importantly, EBF2 was one of the most overexpressed genes (R fold 5.75 and $P = 8.62 \times 10^{-5}$) in osteosarcoma compared with controls.

Ingenuity pathways

To elucidate the pathways altered in osteosarcoma, we performed network clustering of previously validated genes using the Ingenuity Software tool. Several significant networks were established with different scores (Supplementary Fig. S4). The most significant network includes 19 different genes functionally related with proliferation, cell death, and cancer. Among them, TNFRSF6, a decoy receptor for Fas ligand, which belongs to the main hub in this network, has been previously implicated in osteoblast differentiation survival and apoptosis (24).

Characterization of TRAIL pathway

EBF2 was one of the most significantly overexpressed genes in the osteosarcoma signature and it has been shown to act as transactivator of OPG in osteoblasts (14). We analyzed the OPG expression levels in an independent set of samples ($P < 0.028$; Fig. 3). Osteosarcoma-derived cell lines secreted higher levels of OPG compared with control paired cells ($P < 0.009$). More importantly, ELISA assessment of OPG in conditioned medium of tumor cells was markedly increased compared with normal osteoblasts (Fig. 3). Of note, no such differences were found in populations with mutations in TP53. To validate these findings in an independent set of samples, we performed inmunohistochemistry in a osteosarcoma tissue microarray. Immunohistochemical analysis of a tissue microarray using an anti-EBF2 antibody revealed immunoreactivity in ~70% of osteosarcoma samples. EBF2 staining was predominantly nuclear despite strong cytoplasmic immunoreactivity (Fig. 3C). There was not correlation between staining intensity and prognosis (data not shown).

To assess the direct involvement of EBF2 in OPG expression, we lentivirally transduced a high-expressing OPG osteosarcoma cell line (595B) with a short hairpin RNA targeting EBF2 to reduce EBF2 expression levels (Fig. 4). Knockdown of EBF2 reduced mRNA levels ~50% to 70% compared with vector and control cells. We quantified OPG levels in the conditioned medium of these cell lines by ELISA. Interestingly, OPG levels were significantly reduced in EBF2 knockdown cells compared with vector and control cell lines (Fig. 4). These data indicate that increased levels of EBF2 transcription factor could be partially mediating OPG up-regulation in osteosarcoma cells.

We then studied the implications of OPG levels in conditions of TRAIL-induced apoptosis. In the absence of OPG, the number of cells was decreased 48 h after treatment with TNF-α and TRAIL. In contrast, incubation with OPG substantially increased the survival after the proapoptotic induction with TNF-α or TRAIL alone (Fig. 4). We analyzed whether the previous effects on proliferation were due to apoptosis. Caspase-3 and -7 activities were increased after treatment with TNF-α and TRAIL. Interestingly, incubation with OPG dramatically decreased caspase activities of TRAIL-treated cells, whereas it displayed a residual effect on TNF- α-treated cells. Taken together, these data indicate that high OPG levels showed a protective effect in TRAIL-induced apoptosis, preventing activation of downstream caspase-3/7 activities.

DISCUSSION

In this report, we have identified a transcriptomic signature by isolating chemonaive tumor-derived cell populations from patients diagnosed with sporadic osteosarcoma. Among this gene subset, the transcription factor EBF2 was found up-regulated in tumor samples. Similarly, its downstream target OPG, a RANK decoy receptor involved in osteoclast activation, showed higher expression levels in osteosarcoma-derived samples than paired control cells. More importantly, relative RANKL/OPG expression levels were lower in osteosarcoma samples than in normal osteoblasts (Supplementary Fig. S5). Thus, in the context of osteosarcoma, OPG overexpression may inhibit osteoclastogenesis, tilting the balance of bone turnover and favoring aberrant bone formation.

Recently, in normal bone homeostasis, Kieslinger et al. showed that OPG was transcriptionally up-regulated by EBF2 (14). In contrast, OPG up-regulation in osteosarcoma did not totally correlate with EBF2 expression levels for all samples, suggesting other mechanisms of OPG regulation. Interestingly, Wnt signaling pathway, which has been found altered in osteosarcoma (25, 26), could strongly synergize with EBF2 to induce OPG (14). In this regard, several Wnt signaling components were deregulated in our gene signature. Similarly, samples harboring TP53 mutations displayed normal OPG levels despite their high EBF2 expression. This finding was intriguing because p53 knockout mice display higher levels of OPG. In contrast, activation of p53 led to a down-regulation of OPG in endothelial cells (27). Therefore, OPG up-regulation might involve other EBF2-independent mechanisms as suggested previously (28).

Besides a role in normal bone homeostasis, OPG also acts as a decoy receptor for the cytotoxic effects induced by TRAIL in a variety of tumor cells with little effect on normal cells. TRAIL binds to its transmembrane receptors DcR4 and DcR5, which are expressed in normal and malignant cells. In addition to OPG, DcR1 and DcR2, which lack their intracellular death domain, act as decoy receptors preventing TRAIL-induced apoptosis. Both are highly expressed in normal cells but are almost absent in tumor cells (27).

According to our findings, the ability of OPG to inhibit TRAIL-induced apoptosis might represent an important mechanism in promoting tumor cell survival. Indeed, TRAIL alone or in combination with radiotherapy and chemotherapy sensitizes tumor cells to apoptosis in osteosarcoma (29). In many other tumors (30, 31), OPG represents a

survival factor in a TRAIL-independent manner and its overexpression increases cell proliferation and tumor growth in vivo (32).

Paradoxically, recombinant OPG-Fc treatment in osteosarcoma models showed therapeutic benefits by blocking the RANK/RANKL system in the bone microenvironment and preventing tumor-induced osteolysis, without affecting tumor cell survival (33). This apparent discrepancy with our findings could be explained by the use of OPG truncated protein that lacks the death domains, the heparin-binding domain, and the dimerization sequences, which are required for the intracellular actions. One could speculate that specific OPG blocking antibodies against these domains could inhibit osteosarcoma-secreted OPG, potentiating TRAIL-mediated apoptosis (32). Besides OPG, other mechanisms involving prosurvival Bcl-2 proteins, such as Mcl-1, have been implicated in TRAIL resistance (34–36). Therefore, combined treatment targeting different mechanisms of TRAIL resistance could theoretically increase apoptotic response in vitro and improve clinical benefit. These speculations, however, need to be experimentally addressed in relevant animal models. Indeed, in vivo findings emphasize the tumor-inhibitory effect of a truncated OPG by blocking the RANK/RANKL axis (33, 37). These effects would be dependent on the relative concentrations, timing, and location of OPG, TRAIL, and RANKL expression in the bone microenvironment influenced by both normal and tumor cell types (38). Therefore, only by determining their in vitro expression levels in tumor cells would be difficult to anticipate the net balance of these players in the in vivo microenvironment.

Our strategy circumvented several obstacles to discern the expression profile of transformed osteosarcoma cells specifically dissecting cell-autonomous effects. By isolating transformed cell populations, we avoided confounding effects of the surrounding stroma and inflammatory tissue, thus obviating non-cell-autonomous effects. In addition, the enrichment of the sample for tumor cells by serial passage (>20), the phenotypic characterization, and the abundant biological material that could be obtained from small diagnostic biopsies represent remarkable advantages over previous strategies. Other technologies such as confocal laser microdissection could facilitate the selection of tumor cells; however, low cellularity of many tumors and the RNA amplification step required are important drawbacks of this approach. In contrast, the isolation of transformed populations in early steps of tumorigenesis is the major advantage, avoiding the accumulation of chromosomal aberrations over time. This is supported by the fact that the comparative genomic hybridization profiling of the primary tumor samples used for the studies included herein revealed almost complete chromosomal integrity (data not shown). In stark contrast, samples isolated from advanced tumors showed a panoply of karyotypic alterations (39).

Our strategy, with the inclusion of nontreated tumors and the use of stringent criteria in the statistical analysis, could partially explain the divergence in the transcriptomic gene signature obtained in other studies (10–13). Instead of focusing in a large collection of specimens with heterogeneous confounding stroma, a small number of homogenous samples derived from sporadic osteosarcoma patients provided strong clustering. The availability of paired-normal osteoblasts for all osteosarcoma patients provided a high-quality control that allowed to minimize intraindividual and interindividual differences and provided further statistical strength. Thus, the identified signature yielded deep differences compared with previously described profiles (10–13). The top discriminators identified by Baird et al. for osteosarcoma (13) were not found in our gene subset. These included PPFIBP2, S100A13, and PTHR1 as well as osteoid-associated genes: P4HA2, PLOD, COL5A1, and LUM. In contrast, members of the

fibroblast growth factor receptor family, such as FGFR1, were also detected in our study. Similarly, one of the clusters found included the Wnt family members, which belong to a key pathway for skeletal and soft-tissue sarcomas (13). Several of the downstream players found among the top 30 discriminators in our analysis include FZD, TLE1, TLE3, and WNT. Perturbation of the Wnt signaling may lead to the abnormal osteoblast differentiation observed in vitro (25, 26).

Nevertheless, some limitations inherent to our technical approach should also be considered. For instance, the isolation of tumor cells from its complex microenvironment might prevent the identification of important genes activated by tumor-stroma interactions such as members of the Notch pathway (40). In addition, this strategy is not adequate to detect key players, such as oncogenes activated by point mutations, or subtle changes in the levels of tumor suppressor genes involved in the carcinogenesis process.

The identification of EBF2 and its validation in an independent set of tumor samples supports the validity of our approach. Future research will be required to further validate many other potential targets identified in this study. This information could be prospectively correlated with the response to chemotherapy or the metastatic outcome. This growing panel of well-characterized tumor-derived cells could also be used for testing novel therapeutics and identifying useful pharmacogenomic profiles that could lead to the use of tailored therapeutic regiments. Similar proof-of-principle could be use to study other pediatric and adult sarcomas.

In summary, we have identified an osteosarcoma gene signature using a novel strategy. This transcriptomic signature revealed a key target EBF2 as commonly up-regulated in human osteosarcoma tumors. Induction of EBF2 could partially account for the OPG overexpression found in tumors and may explain the resistance to TRAIL-induced apoptosis.

DISCLOSURE OF POTENTIAL CONFLICTS OF INTEREST

No potential conflicts of interest were disclosed.

ACKNOWLEDGMENTS

We thank all patients and families who collaborated in our project and N. Ibargoyen, D. Luis-Ravelo, I. Antón, M. Royo, and S. Martínez for outstanding technical assistance.

REFERENCES

1. Fletcher CDM, Unni KK, Mertens F, Organización Mundial de la Salud, International Academy of Pathology, International Agency for Research on Cancer. Pathology and genetics of tumours of soft tissue and bone. Lyon: IARC Press; 2002.
2. Gorlick R, Anderson P, Andrulis I, et al. Biology of childhood osteogenic sarcoma and potential targets for therapeutic development: meeting summary. Clin Cancer Res 2003;9:5442–53.

3. Kansara M, Thomas DM. Molecular pathogenesis of osteosarcoma. DNA Cell Biol 2007;26:1–18.
4. Clark JC, Dass CR, Choong PF. A review of clinical and molecular prognostic factors in osteosarcoma. J Cancer Res Clin Oncol 2008;134: 281–97.
5. Bridge JA, Nelson M, McComb E, et al. Cytogenetic findings in 73 osteosarcoma specimens and a review of the literature. Cancer Genet Cytogenet 1997;95:74–87.
6. Atiye J, Wolf M, Kaur S, et al. Gene amplifications in osteosarcoma—CGH microarray analysis. Genes Chromosomes Cancer 2005; 42:158–63.
7. Sandberg AA, Bridge JA. Updates on the cytogenetics and molecular genetics of bone and soft tissue tumors: osteosarcoma and related tumors. Cancer Genet Cytogenet 2003;145:1–30.
8. Mackall CL, Meltzer PS, Helman LJ. Focus on sarcomas. Cancer Cell 2002;2:175–8.
9. Lecanda F, Avioli LV, Cheng SL. Regulation of bone matrix protein expression and induction of differentiation of human osteoblasts and human bone marrow stromal cells by bone morphogenetic protein-2. J Cell Biochem 1997;67:386–96.
10. Leonard P, Sharp T, Henderson S, et al. Gene expression array profile of human osteosarcoma. Br J Cancer 2003;89:2284–8.
11. Wolf M, El-Rifai W, Tarkkanen M, et al. Novel findings in gene expression detected in human osteosarcoma by cDNA microarray. Cancer Genet Cytogenet 2000;123:128–32.
12. Nielsen TO. Microarray analysis of sarcomas. Adv Anat Pathol 2006;13:166–73.
13. Baird K, Davis S, Antonescu CR, et al. Gene expression profiling of human sarcomas: insights into sarcoma biology. Cancer Res 2005;65: 9226–35.
14. Kieslinger M, Folberth S, Dobreva G, et al. EBF2 regulates osteoblast-dependent differentiation of osteoclasts. Dev Cell 2005;9:757–67.
15. Lecanda F, Warlow PM, Sheikh S, Furlan F, Steinberg TH, Civitelli R. Connexin43 deficiency causes delayed ossification, craniofacial abnormalities, and osteoblast dysfunction. J Cell Biol 2000;151:931–44.
16. Bolstad BM, Irizarry RA, Astrand M, Speed TP. A comparison of normalization methods for high density oligonucleotide array data based on variance and bias. Bioinformatics 2003;19:185–93.
17. Irizarry RA, Bolstad BM, Collin F, Cope LM, Hobbs B, Speed TP. Summaries of Affymetrix GeneChip probe level data. Nucleic Acids Res 2003;31:e15.
18. Irizarry RA, Hobbs B, Collin F, et al. Exploration, normalization, and summaries of high density oligonucleotide array probe level data. Biostatistics 2003;4:249–64.
19. Tusher VG, Tibshirani R, Chu G. Significance analysis of microarrays applied to the ionizing radiation response. Proc Natl Acad Sci U S A 2001;98:5116–21.
20. Benjamini Y, Hochberg Y. Controlling the false discovery rate: a practical and powerful approach to multiple testing. J Roy Stat Soc Ser B 1995;57:289–300.
21. Murtagh F. Multidimensional clustering algorithms: COMPSTAT Lectures 4. Wuerzburg: Phy-sica-Verlag; 1985.
22. Vicent S, Luis-Ravelo D, Anton I, et al. A novel lung cancer signature mediates metastatic bone colonization by a dual mechanism. Cancer Res 2008;68:2275–85.
23. van Maanen JM, Retel J, de Vries J, Pinedo HM. Mechanism of action of antitumor drug etoposide: a review. J Natl Cancer Inst 1988;80: 1526–33.
24. Kovacic N, Lukic IK, Grcevic D, Katavic V, Croucher P, Marusic A. The Fas/Fas ligand system inhibits differentiation of murine osteoblasts but has a

limited role in osteoblast and osteoclast apoptosis. J Immunol 2007;178:3379–89.
25. Hoang BH, Kubo T, Healey JH, et al. Expression of LDL receptor-related protein 5 (LRP5) as a novel marker for disease progression in high-grade osteosarcoma. Int J Cancer 2004; 109:106–11.
26. Hoang BH, Kubo T, Healey JH, et al. Dickkopf 3 inhibits invasion and motility of Saos-2 osteosarcoma cells by modulating the Wnt-β-catenin pathway. Cancer Res 2004;64:2734–9.
27. Secchiero P, Corallini F, Rimondi E, et al. Activation of the p53 pathway down-regulates the osteoprotegerin (OPG) expression and release by vascular endothelial cells. Blood 2008;111: 1287–94.
28. Glass DA II, Bialek P, Ahn JD, et al. Canonical Wnt signaling in differentiated osteoblasts controls osteoclast differentiation. Dev Cell 2005;8: 751–64.
29. Evdokiou A, Bouralexis S, Atkins GJ, et al. Chemotherapeutic agents sensitize osteogenic sarcoma cells, but not normal human bone cells, to Apo2L/TRAIL-induced apoptosis. Int J Cancer 2002;99:491–504.
30. Holen I, Croucher PI, Hamdy FC, Eaton CL. Osteoprotegerin (OPG) is a survival factor for human prostate cancer cells. Cancer Res 2002; 62:1619–23.
31. Holen I, Cross SS, Neville-Webbe HL, et al. Osteoprotegerin (OPG) expression by breast cancer cells in vitro and breast tumours in vivo—a role in tumour cell survival? Breast Cancer Res Treat 2005;92:207–15.
32. Fisher JL, Thomas-Mudge RJ, Elliott J, et al. Osteoprotegerin overexpression by breast cancer cells enhances orthotopic and osseous tumor growth and contrasts with that delivered therapeutically. Cancer Res 2006;66: 3620–8.
33. Lamoureux F, Richard P, Wittrant Y, et al. Therapeutic relevance of osteoprotegerin gene therapy in osteosarcoma: blockade of the vicious cycle between tumor cell proliferation and bone resorption. Cancer Res 2007;67:7308–18.
34. Sinicrope FA, Penington RC, Tang XM. Tumor necrosis factor-related apoptosis-inducing ligand-induced apoptosis is inhibited by Bcl-2 but restored by the small molecule Bcl-2 inhibitor, HA 14-1, in human colon cancer cells. Clin Cancer Res 2004;10:8284–92.
35. Sun SY, Yue P, Zhou JY, et al. Overexpression of BCL2 blocks TNF-related apoptosis-inducing ligand (TRAIL)-induced apoptosis in human lung cancer cells. Biochem Biophys Res Commun 2001;280:788–97.
36. Ricci MS, Kim SH, Ogi K, et al. Reduction of TRAIL-induced Mcl-1 and cIAP2 by c-Myc or sorafenib sensitizes resistant human cancer cells to TRAIL-induced death. Cancer Cell 2007;12:66–80.
37. Lamoureux F, Picarda G, Garrigue-Antar L, et al. Glycosaminoglycans as potential regulators of osteoprotegerin therapeutic activity in osteosar-coma. Cancer Res 2009;69:526–36.
38. Shipman CM, Croucher PI. Osteoprotegerin is a soluble decoy receptor for tumor necrosis factor-related apoptosis-inducing ligand/Apo2 ligand and can function as a paracrine survival factor for human myeloma cells. Cancer Res 2003;63:912–6.
39. Selvarajah S, Yoshimoto M, Ludkovski O, et al. Genomic signatures of chromosomal instability and osteosarcoma progression detected by high resolution array CGH and interphase FISH. Cytogenet Genome Res 2008;122:5–15.
40. Engin F, Yao Z, Yang T, et al. Dimorphic effects of Notch signaling in bone homeostasis. Nat Med 2008;14:299–305.

Grant support: Spanish Ministry of Health/FIS grant PI040010 and Government of Navarra grant 17/2004 (A. Patiño-García); "UTE project FIMA" agreement; Spanish Ministry of Health/FIS Feder (RTICCC C03/10) grant PI070031 (F. Lecanda); and Spanish Ministry of Industry, Tourism and Commerce grant FIT-090100-2005-46. F. Lecanda is an investigator from I3 Program.

Current address for G. Toledo: Department of Pathology, M. D. Anderson International, Madrid, Spain.

Requests for reprints: Fernando Lecanda, Division of Oncology, Adhesion and Metastasis Laboratory, Center for Applied Biomedical Research, University of Navarra, E31080 Pamplona, Spain. Phone: 34-948-194-700, ext. 1001. Fax: 34-948-194-714; E-mail: flecanda@unav.es.

Table 1. Clinical, histopathologic, and molecular features of the osteosarcoma patients and tumor samples

Patient	Histology	x-ray appearance	Age (y)	Gender	Location	Necrosis	Follow-up	Survival (mo)	Event-free survival (mo)	TP53 status
473	Fibroblastic	Osteolytic	15.08	M	Tibia	95%	Remission	74	66	Normal
475	Osteoblastic	Osteoblastic	23.5	F	Femur	100%	Remission	74	68	Normal
486	Osteochondroblastic	Osteoblastic	24	M	Tibia	NA*	Died of disease	14	0	Loss of heterozygosity/ S241Y
491	Osteochondroblastic	Osteoblastic	16.6	M	Femur	90%	Progression	69	20	Normal
500	Osteoblastic	Osteolytic	11	M	Femur	>90%	Remission	68	59	Normal
524	Osteochondroblastic	Osteoblastic	11	F	Femur	<10%	Remission	72	56	Normal
531	Osteochondroblastic	Osteoblastic	22	F	Multifocal	85%	Died of disease	27	0	Loss of heterozygosity/ C277Y

*NA, not available.

Table 2. Genes that were (P < 0.05) or tended to be (P = 0.05-0.09) differentially expressed in osteosarcomas cells compared with normal osteoblasts, further validated by Micro Fluidic Cards

Probe-set ID	TaqMan Assay	Gene symbol	Gene name	P	Fold change
214782_at	Hs00193322_m1	CTTN	Cortactin	0.0003	1.47
200685_at	Hs00191108_m1	SFRS11	Splicing factor, arginine/serine-rich 11	0.0003	1.73
206187_at	Hs00168765_m1	PTGIR	Prostaglandin I2 (prostacyclin) receptor (IP)	0.0004	6.03
205105_at	Hs00159007_m1	MAN2A1	Mannosidase, a, class 2A, member 1	0.0006	2.55
200668_s_at	Hs00704312_s1	UBE2D3	Ubiquitin-conjugating enzyme E2D 3	0.0006	1.71
218026_at	Hs00360235_m1	HSPC009	HSPC009 protein	0.0012	1.56
209708_at	Hs00378239_m1	MOXD1	Monooxygenase, DBH-like 1	0.0012	11.39
203221_at	Hs00270768_m1	TLE1	Transducin-like enhancer of split 1	0.0012	2.62
218517_at	Hs00368739_m1	PHF17	PHD finger protein 17	0.0014	2.69
201487_at	Hs00175188_m1	CTSC	Cathepsin C	0.0016	5.35
201578_at	Hs00193638_m1	PODXL	Podocalyxin-like	0.0023	49.60
202410_x_at	Hs00171254_m1	IGF2	Insulin-like growth factor 2 (somatomedin A)	0.0024	0.36
221901_at	Hs00286734_m1	KIAA1644	KIAA1644 protein	0.0025	0.36
201701_s_at	Hs00175051_m1	PGRMC2	Progesterone receptor membrane component 2	0.0025	2.22
213885_at	Hs00197678_m1	TRIM3	Tripartite motif-containing 3	0.0025	1.43
206702_at	Hs00176096_m1	TEK	TEK tyrosine kinase, endothelial	0.0030	11.76
215029_at	Hs00607590_m1	FLJ12666	Hypothetical protein FL]12666	0.0040	1.37
221586_s_at	Hs00231092_m1	E2F5	E2F transcription factor 5, p130-binding	0.0046	0.67
200745_s_at	Hs00181845_m1	GNB1	Guanine nucleotide binding protein, β polypeptide 1	0.0053	1.37
213517_at	Hs00245320_m1	PCBP2	Poly(rC) binding protein 2	0.0062	1.58
210648_x_at	Hs00601001_m1	SNX3	Sorting nexin 3	0.0071	1.80
222282_at	Hs00406243_m1	PAPD4	PAP-associated domain containing 4	0.0081	1.30
220392_at	Hs00224081_m1	EBF2	Early B-cell factor 2	0.0084	13.64
213593_s_at	Hs00203263_m1	TRA2A	Transformer-2a	0.0093	1.47
205803_s_at	Hs00608195_m1	TRPC1	Transient receptor potential cation channel, subfamily C, member 1	0.0093	1.53
215588_x_at	Hs00187143_m1	RIOK3	RIO kinase 3 (yeast)	0.0107	1.63
201722_s_at	Hs00234919_m1	GALNT1	UDP-N-acetyl-a-D-galactosamine	0.0122	0.61
208200_at	Hs00174092_m1	IL1A	Interleukin 1, a	0.0128	18.93
213015_at	Hs00220317_m1	BBX	Bobby sox homologue (Drosophila)	0.0139	1.61
203881_s_at	Hs00187805_m1	DMD	Dystrophin (muscular dystrophy, Duchenne and Becker types)	0.0158	4.90
212672_at	Hs00175892_m1	ATM	Ataxia telangiectasia mutated	0.0179	1.54
213791_at	Hs00175049_m1	PENK	Proenkephalin	0.0192	0.32
212492_s_at	Hs00392119_m1	JMJD2B	]umonji domain containing 2B	0.0203	1.38
200769_s_at	Hs00428515_g1	MAT2A	Methionine adenosyltransferase II, a	0.0229	1.47
205518_s_at	Hs00379137_m1	CMAH	CMP-N-acetylneuraminic acid hydroxylase	0.0258	3.72
35436_at	Hs00366395_m1	GOLGA2	Golgi autoantigen, golgin subfamily a, 2	0.0259	1.33
203181_x_at	Hs00177301_m1	SRPK2	SFRS protein kinase 2	0.0259	2.25
209678_s_at	Hs00702254_s1	PRKCI	Protein kinase C, iota	0.0291	1.17
204471_at	Hs00176645_m1	GAP43	Growth-associated protein 43	0.0298	0.79
220046_s_at	Hs00220399_m1	CCNL1	Cyclin L1	0.0327	1.85
207365_x_at	Hs00739382_m1	WDR45	WD repeat domain 45	0.0350	1.59
207186_s_at	Hs00189461_m1	FALZ	Fetal Alzheimer antigen	0.0459	1.76
210407_at	Hs00221372_m1	PPM1A	Protein phosphatase 1A, magnesium-dependent, a isoform	0.0459	1.49
208620_at	Hs00362410_s1	PCBP1	Poly(rC) binding protein 1	0.0570	1.29
205522_at	Hs00429605_m1	HOXD4	Homeobox D4	0.0671	1.99
206472_s_at	Hs00183222_m1	TLE3	Transducin-like enhancer of split 3	0.0702	0.78
204341_at	Hs00414879_m1	TRIM16	Tripartite motif-containing 16	0.0702	0.84
215404_x_at	Hs00241111_m1	FGFR1	Fibroblast growth factor receptor 1	0.0777	1.48
208502_s_at	Hs00267528_m1	PITX1	Paired-like homeodomain transcription factor 1	0.0917	0.91

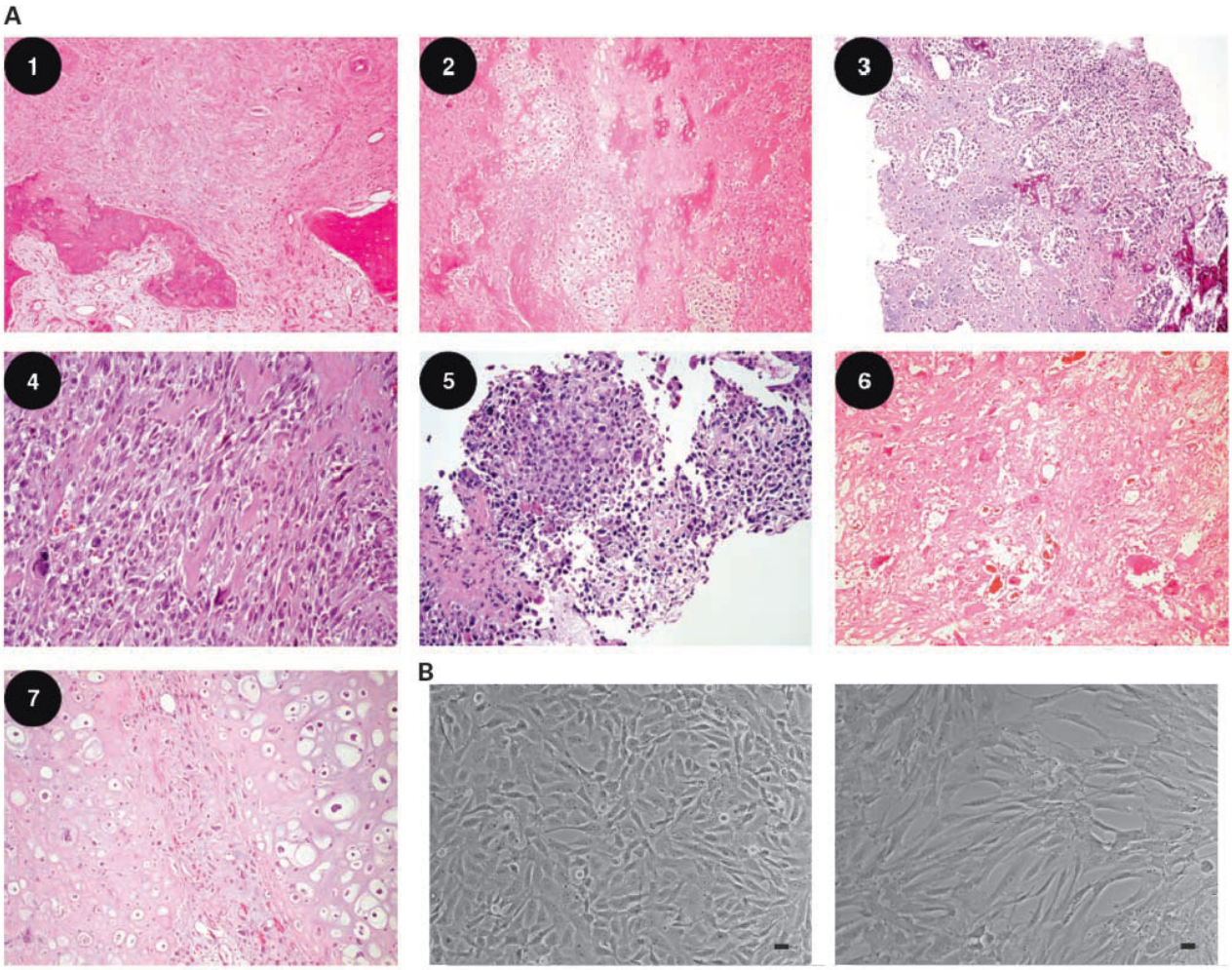

Figure 1. Histologic features of the tumors at diagnosis and morphology of derived cells in culture. **A**, histologic appearance of the tumor samples at diagnosis. **B**, representative morphology of two cell populations established in vitro from different tumors (left, 531 cells; right, 473 cells). Bar, 25 μm. 1. Patient #473; 2. Patient #475; 3. Patient #486; 4. Patient #491; 5. Patient #500; 6. Patient #524; 7. Patient #531.

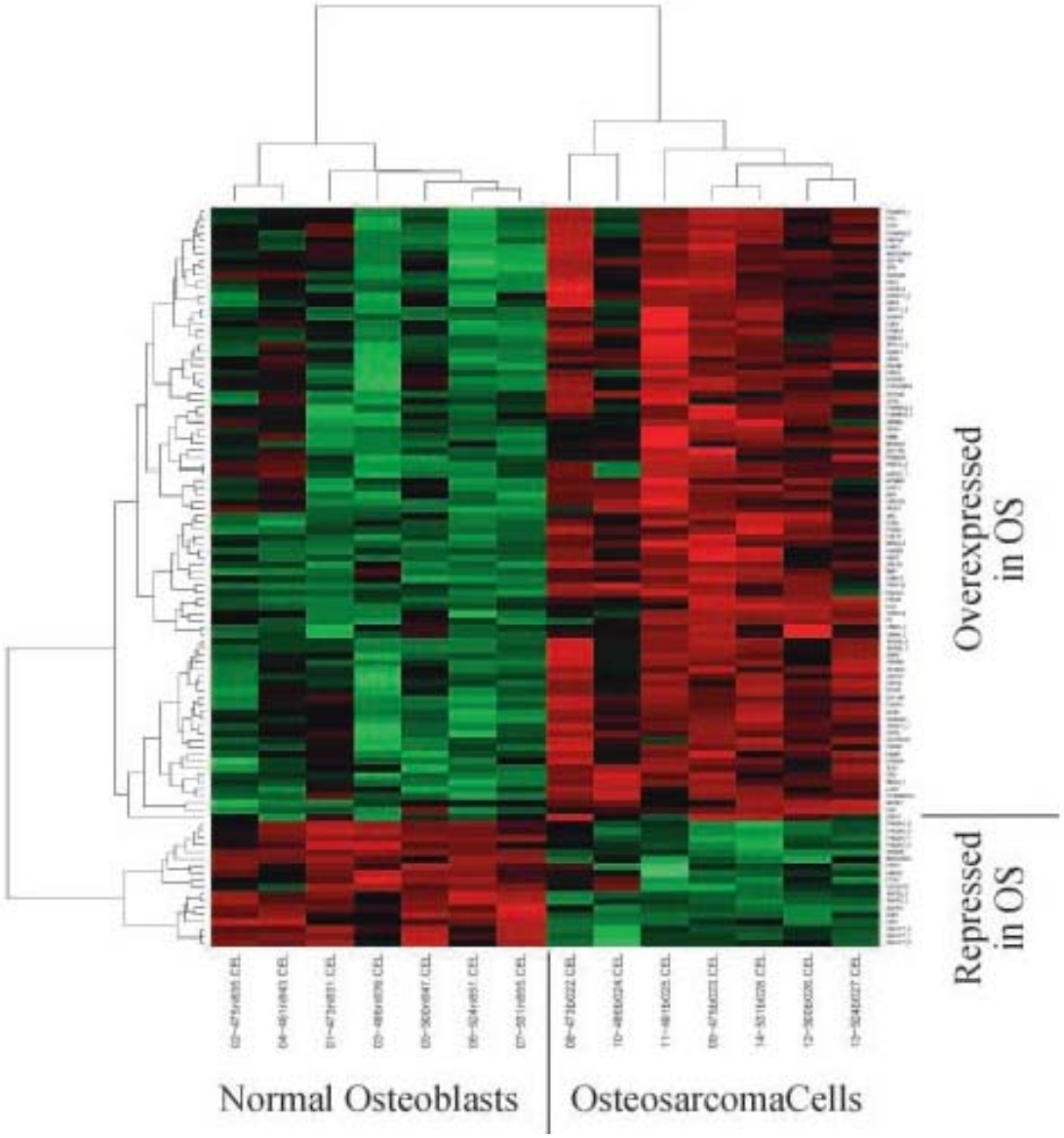

Figure 2. Hierarchical cluster diagram of differentially expressed genes in primary osteosarcoma cell populations versus paired-normal osteoblasts. Rows, single-gene probe-sets; columns, results from the single-microarray hybridizations. Each box is the hybridization signal value of a gene probeset in the microarray assay. The intensity of the color saturation in each probe-set box (ranging from 2 to 14 in $\log_2$ scale) provides a quantitative estimation of its expression level (red, overexpression; green, repression).

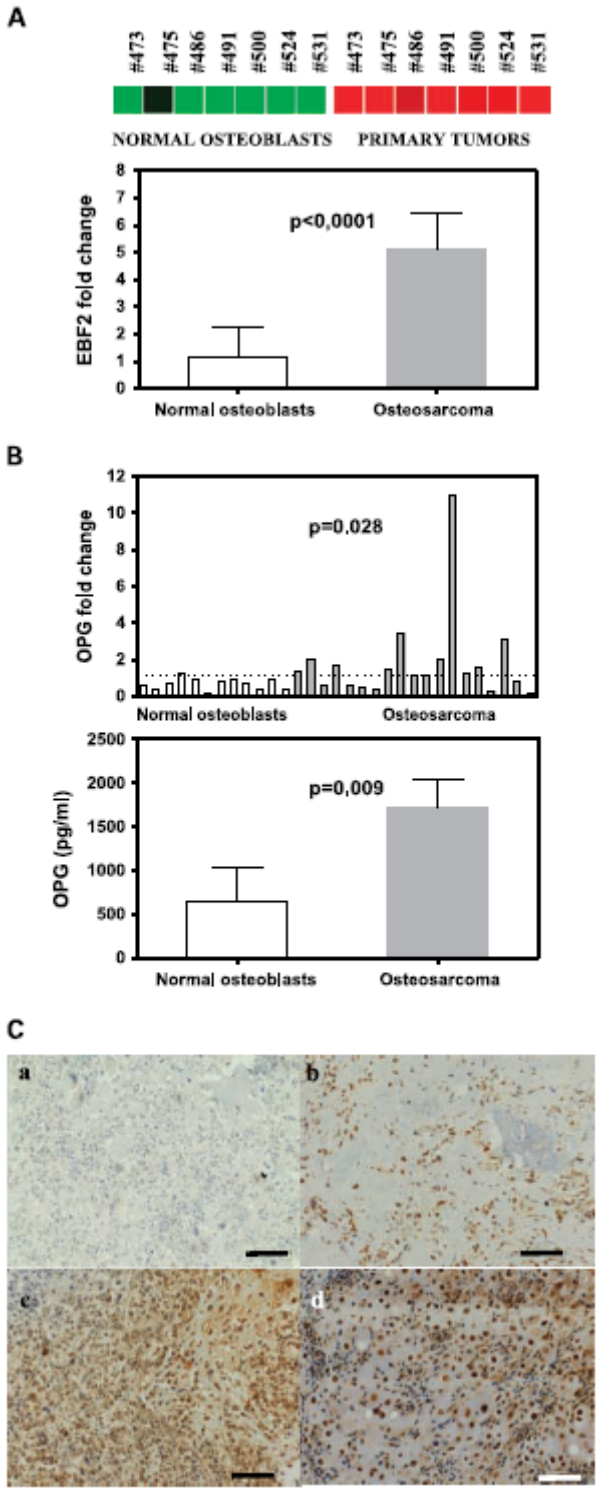

Figure 3. A, detailed diagram of the microarray hybridization signals for the probe-set (220392_at) corresponding to the EBF2 gene in osteosarcoma paired control samples and quantitative RT-PCR for EBF2 in an independent set of osteosarcoma and normal osteoblast samples (n = 12). **B**, top, quantitative RT-PCR results for OPG expression levels; bottom, OPG protein levels in the conditioned medium of independent samples (control: n = 12 and osteosarcoma: n = 12) were analyzed by ELISA. **C**, representative images of immunohistochemical analysis of EBF2 in osteosarcoma sections. b to d, high intensity of staining; a, almost complete absence of immunoreactivity. Bar, 100 μm.

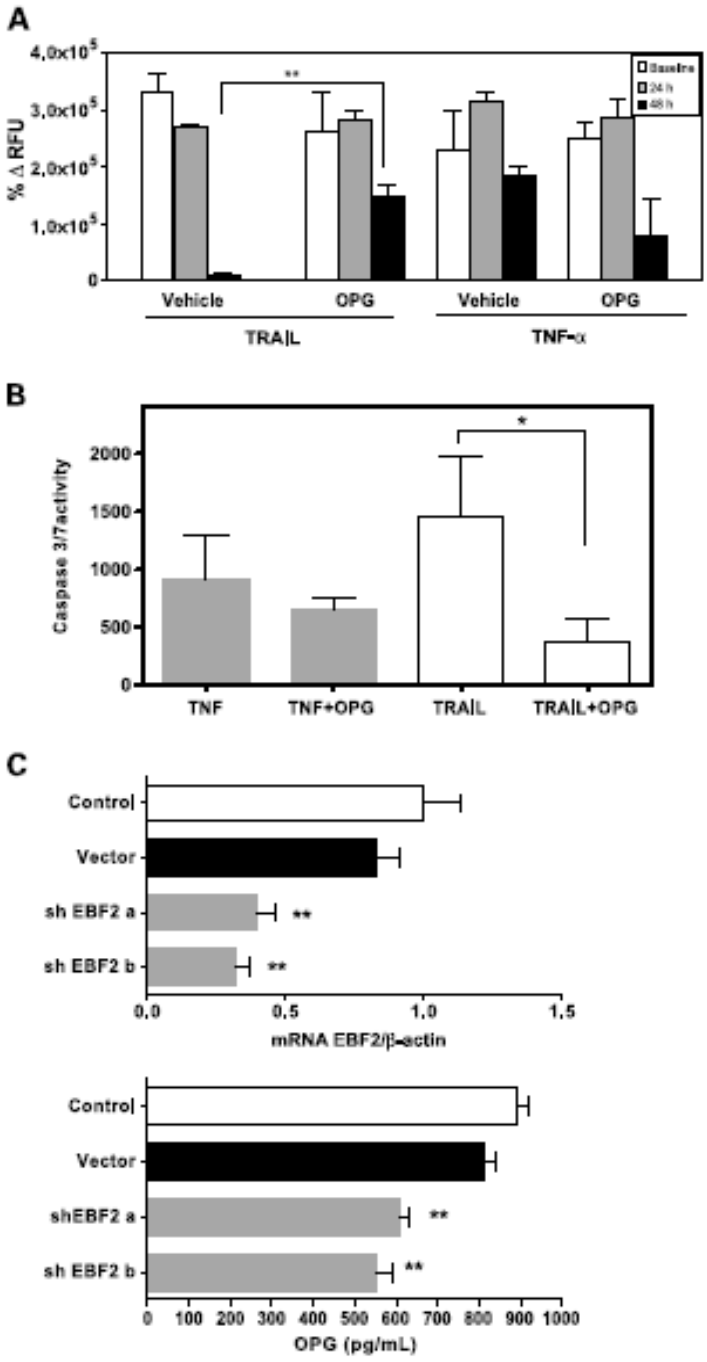

Figure 4. A, proliferation of osteosarcoma cells assessed by the MTT assay in the presence or absence of OPG after incubation for 48 h with TNF-α (25 ng/ mL), TRAIL (50 ng/mL), or in combination. B, caspase-3/7 activity after 24 h treatment with TNF-α or TRAIL after incubation with OPG (1 μg/mL). C, top, EBF2 silencing after lentiviral transduction of 595B cells with two specific short hairpin RNAs. Levels of EBF2 were quantified by specific RTPCR. Bottom, OPG protein was assessed by ELISA in culture supernatants of two different EBF2-silenced clones compared with control and vector transduced. *, $P < 0.05$; **, $P < 0.001$.